Physica D 243 (2013) 32–44

Contents lists available at SciVerse ScienceDirect

Physica D

journal homepage: www.elsevier.com/locate/physd

Asymptotic analysis of weakly nonlinear Bessel–Gauß beams

Tobias Graf [a,*], Jerome Moloney [a], Shankar Venkataramani [b]

[a] The University of Arizona, Department of Mathematics, Arizona Center for Mathematical Sciences, 617 N. Santa Rita Avenue, Tucson, AZ 85721-0089, USA

[b] The University of Arizona, Department of Mathematics, 617 N. Santa Rita Avenue, Tucson, AZ 85721-0089, USA

ARTICLE INFO

Article history:
Received 2 February 2012
Received in revised form
26 August 2012
Accepted 16 September 2012
Available online 21 September 2012
Communicated by V.M. Perez-Garcia

Keywords:
Conical waves
Nonlinear Schrödinger equation
Multiple scales
Amplitude equations
Uniform estimates

ABSTRACT

In this paper we investigate the propagation of conical waves in nonlinear media. In particular, we are interested in the effects resulting from applying a Gaussian apodization to an ideal nondiffracting wave. First, we present a multiple scales approach to derive amplitude equations for weakly nonlinear conical waves from a governing equation of cubic nonlinear Schrödinger type. From these equations we obtain asymptotic solutions for the linear and the weakly nonlinear problem for which we state several uniform estimates that describe the deviation from the ideal nondiffracting solution. Moreover, we show numerical simulations based on an implementation of our amplitude equations to support and illustrate our analytical results.

1. Introduction

A characteristic feature of wave propagation without waveguides or other boundaries is the phenomenon of *diffraction*, namely the spreading of energy transverse to the direction of propagation. Diffraction compromises the ability of the waves to carry energies over long distances. Nondiffracting waves are thus of considerable practical and theoretical interest and have been studied in various fields such as mathematics, physics, electromagnetics, and optics.

The mathematical analysis of nondiffracting solutions to the linear wave and the Helmholtz equation can be traced back as far as a 1897 paper by Lord Rayleigh [1]. In his work, Lord Rayleigh derives a family of special solutions in terms of Bessel functions for electromagnetic waves traveling in a dielectric cylinder. In 1987, Durnin and others rediscovered these solutions theoretically and experimentally and introduced them as the so-called *Bessel beams* to the optics community; see Durnin [2] and Durnin et al. [3]. Using an appropriate integral representation of the Bessel functions it becomes apparent that these linear Bessel beams belong to the larger family of *conical waves*, since they can be written as a superposition of plane waves whose wave vectors all lie on a cone (see Fig. 1(a)).

Since in a linear medium plane waves are nondiffracting, so too are conical waves. However, this also implies that these ideal nondiffracting solutions have infinite energy and thus cannot be realized experimentally. A physically realizable, finite energy, approximation to these conical waves is obtained by *apodization*, i.e., by introducing a cutoff transverse to the beam propagation. Such apodized Bessel beams will eventually be affected by diffractive effects and can only persist in a finite region; see Fig. 1(b).

A common method in optics to approximate Bessel beams experimentally is described for example by McLeod [4] and McGloin and Dholakia [5]. The main idea consists of focusing a Gaussian beam through a conical lens, called an axicon, which refracts the collimated beam and creates a conical superposition in a finite *Bessel region* behind the lens; see Fig. 2. Theoretically, one can apply a Gaussian apodization to a conical wave to create a finite energy approximation. In the case of the aforementioned Bessel beams, this leads to *Bessel–Gauß* beams; see Gori et al. [6], and Overfelt and Kenney [7]. The concept has been used to study larger families of finite energy approximations for nondiffracting waves, in the linear setting for example by Gutiérrez-Vega and Bandres [8], Bandres and Guizar-Sicairos [9], and Graf et al. [10]. The resilience of conical waves to diffraction makes them interesting objects of study, even in a purely linear setting, with interesting applications in optics and other fields. In particular, special nondiffracting solutions are used frequently as building blocks in *beam engineering* to assemble a beam with certain desirable properties for experiments and applications; see for example Chong et al. [11], McGloin et al. [12], Vasilyeu et al. [13], Lotti et al. [14], as well as Bandres and Gutiérrez-Vega [15,8]. An important question that motivated the research presented in this paper concerns the propagation behavior of such beams in a nonlinear medium. For example, one can ask how the nonlinearity and apodization affect the characteristic

* Corresponding author. Tel.: +1 404 276 4001.
E-mail address: tbgraf@gmail.com (T. Graf).

0167-2789/$ – see front matter © 2012 Elsevier B.V. All rights reserved.
doi:10.1016/j.physd.2012.09.004

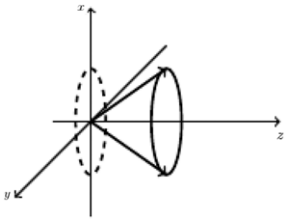

(a) Conical waves are superpositions of plane waves whose wave vectors all lie on the surface of a cone. However, they are unphysical since they carry infinite energy.

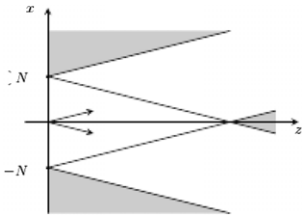

(b) A finite energy conical wave can be viewed as a superposition of apodized plane waves. The finite conical region where the waves interfere to create an almost nondiffracting beam is often referred to as the Bessel region.

Fig. 1. Infinite and finite energy conical waves.

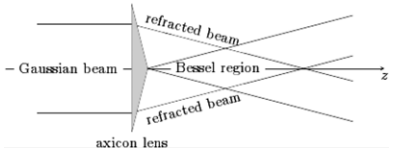

Fig. 2. A Gaussian beam propagating in the positive z-direction is refracted by an axicon lens. The double cone region where the resulting plane waves interfere to form a conical wave is often referred to as the Bessel region.

features of the beam, especially the preservation of the transverse profile and the resilience to diffraction; see Bandres and Gutiérrez-Vega [15,8], Johannisson et al. [16], and Lotti et al. [14].

In this paper we present various uniform estimates that provide, among other results, bounds for the deviation of an asymptotic finite energy solution from an ideal nondiffracting solution. These estimates can be derived from a fairly general multiple scales approach that we apply in the linear and nonlinear setting and which can also be used to develop numerical methods for simulations and computer experiments. Our approach is based on the asymptotic analysis of special solutions for a governing partial differential equation (PDE) of nonlinear Schrödinger type. Although nonlinear nondiffracting waves have been studied before, for example by Johannisson et al. [16] using variational methods, to the best of our knowledge the current PDE based approach and in particular the resulting uniform estimates have not been previously described.

We start by stating the following problem. Consider the following initial value problem (IVP) in cylindrical coordinate system (r, θ, z).

$$-i\frac{\partial \mathcal{A}}{\partial z} = \frac{1}{2k_z}\Delta_\perp \mathcal{A} + n_2 I k_z \mathcal{A} \tag{1.1}$$

$$\mathcal{A}(r, \theta, 0) = E_0\, e^{-\frac{r^2}{L^2}}\, J_n\big(k_\perp r\big)\, e^{in\theta}. \tag{1.2}$$

In the above equations, n is a positive integer and J_n the nth order Bessel function.

$\mathcal{A}$ represents the (complex) amplitude of the electric field, n_2 is the second order nonlinear index of refraction (the Kerr coefficient) and I the intensity (irradiance) given by $I = cn_0\epsilon_0|\mathcal{A}|^2/2$ where c is the speed of light, n_0 is the refractive index of the medium and ϵ_0 is the vacuum permittivity. Since $I \propto |\mathcal{A}|^2$, Eq. (1.1) is the dispersionless Nonlinear Schrödinger (NLS) equation [17]. We consider the case of $n_2 > 0$ which corresponds to the focusing NLS. k_z is the longitudinal wave number and $k_\perp$ is the transverse wavenumber.

Eq. (1.2) describes the initial condition for the NLS equation, in the form of a Bessel function. E_0 is the peak electric field for $n = 0$, and for other n, it sets the scale of the electric field. The width of the Gaussian apodization is controlled by the length scale $L > 0$. In the above, the right-hand side of (1.2) corresponds to the initial conditions for a nth-order Bessel beam. In the rest of the paper we often use the integral representation

$$\mathcal{A}(r, \theta, 0) = \frac{E_0}{2\pi i^n}\, e^{-\frac{r^2}{L^2}} \int_0^{2\pi} e^{ia(x\cos(\phi)+y\sin(\phi))}\, e^{in\phi}\, \mathrm{d}\phi,$$

where $x = r\cos\theta, y = r\sin\theta$ are the cartesian coordinates of a point with cylindrical coordinates (r, θ, z). Furthermore, our discussion is mainly for the zeroth order Bessel beam ($n = 0$), but the results can be extended to the more general case for positive integers n. Note that throughout this paper we suppress the harmonic time dependence of the solutions for brevity.

The goal of this paper is to derive amplitude equations for asymptotic solutions to the IVP above and, most importantly, state uniform estimates for these asymptotic solutions that compare them to the ideal nondiffracting solution. Thus, we obtain theoretical confirmations of experimental observations and geometric optics arguments concerning the geometry of the Bessel region. Moreover, we obtain in some cases new geometries that to our knowledge have not been discussed in the literature previously.

There are several reasons to study problems of the form (1.1), (1.2) in the nonlinear as well as the linear setting. Linear Schrödinger type equations arise frequently in applied mathematics and other fields as paraxial approximations of wave propagation models; see for example Bamberger et al. [18,19], Grella [20]. In optics for example they arise in a PDE framework for diffraction phenomena that is equivalent to the frequently used Kirchhoff integrals [20]. Similarly, the cubic NLS equation arises in nonlinear optics as a model for diffraction and Kerr effects, as well as a model for nonlinear wave propagation in fluid dynamics; see Sulem and Sulem [21], Moloney and Newell [17], and Miller [22], as well as Lotti et al. [14].

Remark 1.1 (*Paraxial Equation*)**.** A linear Schrödinger equation (often referred to as paraxial or paraxial wave equation) arises as a model for diffraction in the paraxial limit for a linear medium in optics; see Grella [20] and references therein. Here, we sketch a heuristic argument for the derivation of the linear Schrödinger equation from the Helmholtz equation in the paraxial limit. We start with the Helmholtz equation

$$\big(\Delta + {\omega_0}^2\big)\, u(x, y, z) = 0 \tag{1.3}$$

where $\omega_0 \in \mathbb{R}$. Applying Fourier transforms with respect to x, y, and z we obtain the dispersion relation

$$-{k_x}^2 - {k_y}^2 - {k_z}^2 + {\omega_0}^2 = 0.$$

Furthermore, we make a paraxial approximation and assume that the direction of propagation is close to the z axis, that is ${k_x}^2+{k_y}^2 \approx 0$. Next, we put

$$u(x,y,z) = v(x,y,z)\exp(ik_z z)$$

and assume v to depend slowly on z. Plugging into the Helmholtz equation (1.3) yields

$$\left(\Delta_\perp v + \underbrace{{\omega_0}^2 v - {k_z}^2 v}_{\approx 0} + 2ik_z\partial_z v + \underbrace{\partial_{zz} v}_{\approx 0}\right)\exp(ik_z z) = 0$$

where $\Delta_\perp$ denotes the transverse Laplacian with respect to x and y. Neglecting the small terms we obtain for v the linear Schrödinger equation

$$\Delta_\perp v(x,y,z) = -2ik_z\partial_z v(x,y,z).$$

As we have mentioned earlier conical waves, and in particular Bessel beams, have been of tremendous interest in recent years to theorists and experimentalists alike, for example because of the property that they preserve their transverse profile during linear propagation.

Remark 1.2 (*Linear Bessel Beams*)**.** We can derive a solution for the linear paraxial equation

$$-i\frac{\partial u}{\partial z}(x,y,z) = \Delta_\perp u(x,y,z) \tag{1.4}$$

using a separation of variables ansatz in cylindrical coordinates

$$u(\mathbf{x}) = v(r(x,y))w(z). \tag{1.5}$$

Note that we assume rotational symmetry with respect to the z-axis (propagation direction) and therefore use cylindrical coordinates (r,θ,z), where $r(x,y) = \sqrt{x^2+y^2}$. Plugging (1.5) into Eq. (1.4) and separating variables yield for some constant a the following Bessel type differential equation for v

$$r^2\, v''(r) + r\, v'(r) + a^2\, r^2\, v(r) = 0. \tag{1.6}$$

A solution of (1.6) is given by $v(r) = J_0(ar)$, where J_0 denotes the zeroth order Bessel function of the first kind; see also Lord Rayleigh [1], Durnin [2] for a related discussion for the wave equation. Furthermore, we obtain for the second factor in (1.5) that $w(z) = \exp(-ia^2 z)$. Hence, a solution of (1.4) is given by the zeroth order Bessel beam

$$u(x,y,z) = J_0\left(a\sqrt{x^2+y^2}\right)\exp(-ia^2 z).$$

Note that in the present paper we will be mostly concerned with the integral representation

$$\frac{1}{2\pi}\int_0^{2\pi} e^{ia(x\cos(\phi)+y\sin(\phi))}\,\mathrm{d}\phi\ \exp(-ia^2 z) = J_0\left(a\sqrt{x^2+y^2}\right)\exp(-ia^2 z)$$

to describe Bessel beams. As mentioned before, this integral is simply a superposition of plane waves whose wave vectors all lie on the boundary of a cone; hence Bessel beams are a special class of *conical waves*. Moreover, if we allow the solution to vary in the angular direction of ϕ, we obtain higher order Bessel beams corresponding to the Bessel functions J_n for positive integers n. More precisely, we obtain solutions of the form

$$\frac{(-i)^n}{2\pi}\int_0^{2\pi} e^{in\phi}\, e^{ia(x\cos(\phi)+y\sin(\phi))}\,\mathrm{d}\phi\ \exp(-ia^2 z) = J_n(ar)\, e^{in\theta}\ \exp(-ia^2 z)$$

where (r,θ,z) are again cylindrical coordinates.

Problem (1.1), (1.2) was formulated for the practically important case of two transverse dimensions (1+2D). Another interesting extension of this model would also include dispersive effects through a time derivative; we plan to return to this case in a separate paper. However, it is curious to point out that even the seemingly simple case with only one transverse dimension (1+1D) can offer interesting new results and insights, as has been shown in case of the discovery of 1+1D Airy waves by Berry and Balazs [23] and the subsequent studies by Bandres and Gutiérrez-Vega [15], and Lotti et al. [14]. Higher dimensional analogues, the so-called *Airy beams*, are currently a very active research area with interesting applications, for example in nanotechnology and beam engineering (Dholakia and Cizmar [24], Siviloglou et al. [25], and McGloin et al. [12]). In recent years there has been a number of innovative theoretical beams that have been engineered with interesting properties in mind. A logical question is then to ask in which way these characteristics are preserved or altered when one introduces an apodization in the problem to create a finite energy wave or when nonlinear effects are taken into account. In this paper we will develop a multiple scales framework for the NLS equation (1.1) that allows us to consider diffractive effects arising from a Gaussian apodization and nonlinear effects simultaneously. We obtain sets of amplitude equations and asymptotic solutions for which we state several uniform estimates that describe rigorously the deviations from the ideal nondiffracting beams.

This paper is organized as follows. In Section 2 we introduce a multiple scales framework which we apply to derive a set of amplitude equations and corresponding asymptotic solutions. In Section 3 we present our main results in form of uniform estimates for asymptotic solutions in the linear and the nonlinear case. The statements contain very characteristic geometric regions on which the estimates hold. These are in good qualitative agreement with the geometric optics description and experimental observation of the Bessel region. Moreover, some of our estimates actually extend to a region that cannot be explained with the geometric optics approximation of light ray propagation but instead results from a difference in phase and group velocity in the wave description. In Section 4 we reduce the problem to the case of one transverse dimension and compare the solutions of our amplitude equations and the governing NLS equation to support our analytical results. The latter section also discusses possible applications for numerical simulations. In the final section we summarize the previous results and discuss potential extensions and applications.

2. Amplitude equations

In this section we describe a perturbative framework for the derivation of asymptotic solutions to the IVP (1.1), (1.2). Eqs. (1.1) and (1.2) are written in dimensional units, so we first begin by nondimensionalizing these equations. We nondimensionalize all the lengths in the problem by the longitudinal wavenumber k_z. Denoting nondimensional quantities with a tilde, we define

$$\tilde r = 2k_z r, \qquad \tilde z = 2k_z z, \qquad \tilde x = 2k_z x, \qquad \tilde y = 2k_z y.$$

In terms of the nondimensional lengths, we have

$$\frac{\partial}{\partial z} = 2k_z\frac{\partial}{\partial \tilde z}, \qquad \Delta_\perp = 4k_z^2\tilde\Delta_\perp.$$

We define $\mathcal{A} = E_0 u$, where E_0 is the peak electric field, so that u is a non-dimensional electric field. Since the intensity is proportional to the square of the electric field, we have $I = \beta|u|^2$ where β is a dimensional constant, whose value depends on E_0. Substituting these rescalings in (1.1) yields

$$-i\frac{\partial u}{\partial \tilde z} = \tilde\Delta_\perp u + \frac{n_2\beta}{2}|u|^2 u. \tag{2.1}$$

The linear part of this equation is identical to (1.4). Applying the rescalings to the initial condition (1.2) with $n = 0$ yields

$$u(\tilde{r}, \theta, 0) = J_0(a\tilde{r})e^{-\tilde{r}^2/N^2}$$

where a and N are the nondimensionalization of $k_\perp$ and L respectively, so that

$$a = \frac{k_\perp}{2k_z}, \qquad N = 2k_z L.$$

This definition of a allows us to connect this initial condition to the previously considered solution of (1.6). Finally, we observe that we can determine β in terms of the total power P of the beam. The (dimensional) intensity of the initial condition is given by

$$I = \beta|u(\tilde{r}, \theta, 0)|^2 = \beta I_0 J_0^2(a\tilde{r})e^{-2\tilde{r}^2/N^2}.$$

The total power is obtained by integrating this expression over the transverse profile of the beam so we have

$$P = 2\pi\beta\int_0^\infty J_0^2(a\tilde{r})e^{-2\tilde{r}^2/N^2} r\,\mathrm{d}r = \frac{\pi\beta N^2}{8k_z^2}e^{-\frac{1}{4}a^2N^2} I_0\left(\frac{a^2N^2}{4}\right)$$

where I_0 is the modified Bessel function of the first kind [26]. Note that $aN = k_\perp L$ in terms of the dimensional quantities, and we are interested in the regime where the central lobe of the Bessel beam is much smaller than the radius of the apodization, so that $k_\perp L \gg 1$. Expanding the function I_0 for large values of its argument [26], we obtain

$$P = \sqrt{\frac{\pi}{2}}\frac{\beta N}{4k_z^2 a}.$$

From this expression, we get

$$\beta = \sqrt{\frac{2}{\pi}}\frac{4k_z^2 aP}{N} = \sqrt{\frac{2}{\pi}}\left(\frac{k_\perp P}{L}\right) \tag{2.2}$$

Remark 2.1. With our rescaling, the nondimensional electric field at $r = 0$ is $u = 1$. Consequently the intensity of the Bessel beam at the central peak is β. It is known that every side lobe of the Bessel beam has nearly the same total power [5]. Since the total number of lobes in the apodized beam of radius L is proportional $k_\perp L$, the power per lobe is proportional to $P/(k_\perp L)$. In particular, for the central peak, which has a transverse radius $r_0 \propto 1/k_\perp$, we see that the intensity is given by

$$\beta \propto \frac{P}{k_\perp L}\frac{1}{r_0^2} = \left(\frac{k_\perp P}{L}\right)$$

in agreement with (2.2).

From this point, we will work with the nondimensional equations obtained by the above rescaling. We henceforth drop the tildes on $\tilde{r}, \tilde{z}, \tilde{x}$ and $\tilde{y}$ for clarity of presentation. Using the expression from (2.2) in (2.1), we obtain the dimensionless version of the IVP (1.1), (1.2) as

$$\begin{aligned} -i\frac{\partial u}{\partial z}(x, y, z) &= \Delta_{x,y}u(x, y, z) \pm \epsilon|u|^2u(x, y, z) \\ &= \frac{\partial^2 u}{\partial x^2}(x, y, z) + \frac{\partial^2 u}{\partial y^2}(x, y, z) \\ &\quad \pm \epsilon|u|^2u(x, y, z), \end{aligned} \tag{2.3}$$

$$\begin{aligned} u(x, y, 0) &= \frac{1}{2\pi}e^{-\frac{x^2+y^2}{N^2}}\int_0^{2\pi} e^{ia(x\cos(\phi)+y\sin(\phi))}\,\mathrm{d}\phi \\ &= J_0\big(ar\big)\,e^{-\frac{r^2}{N^2}}. \end{aligned} \tag{2.4}$$

The IVP has 3 dimensionless parameters, namely

$$\epsilon = \frac{1}{\sqrt{2\pi}}\frac{n_2 k_\perp P}{L}, \qquad a = \frac{k_\perp}{2k_z}, \qquad N = 2k_z L.$$

In a typical situation of a laser in air, we have $\lambda = 800$ nm so $k_z \approx 8\times10^6\ \mathrm{m}^{-1}$, $n_2 = 10^{-23}\ \mathrm{m}^2/\mathrm{W}$, $P = 3\times10^{10}\ \mathrm{W}$, $L = 1\ \mathrm{cm} = 10^{-2}$ m, radius of the central lobe $= r_0 = 10\ \mu\mathrm{m}$ and the first zero of J_0 is approximately 2.405 so that $k_\perp \approx 2.4/r_0 = 2.4\times10^5\ \mathrm{m}^{-1}$. Consequently,

$$\epsilon \approx 3\times10^{-6}, \qquad a \approx 1.5\times10^{-2}, \qquad N \approx 1.6\times10^5.$$

ϵ denotes the nondimensional strength of the nonlinearity (with our normalization in terms of the peak electric field) or equivalently the nonlinear change in the refractive index near the central peak. N is a nondimensional measure of the apodization; in particular the number of Bessel rings in the apodized beam is proportional to aN.

We observe that $\epsilon \approx 3\times10^{-6}$ and $N^{-1} \approx 6\times10^{-6}$ are comparable in magnitude and much smaller than one. This observation is key to our analysis as we discuss below.

Remark 2.2. In the above rescaling, the non-dimensional peak electric field is set to 1, and the nonlinear coefficient ϵ is then determined by the parameters of the problem. Alternatively, we can pick the rescaling $\mathcal{A} = \frac{E_0}{\alpha}u$. In this case, the peak amplitude is α, and the same analysis as above yields

$$\epsilon = \frac{1}{\sqrt{2\pi}}\frac{n_2 k_\perp P}{L\alpha^2}.$$

We can now pick α to set ϵ to any desired positive value. In particular, we can pick α to be $O(1)$ and make $\epsilon = N^{-1}$ exactly. Of course, the price we pay is that the initial condition will now read

$$\begin{aligned} u(r, \theta, 0) &= \alpha J_0\big(ar\big)\,e^{-\frac{r^2}{N^2}} \\ &= \frac{\alpha}{2\pi}e^{-\frac{x^2+y^2}{N^2}}\int_0^{2\pi} e^{ia(x\cos(\phi)+y\sin(\phi))}\,\mathrm{d}\phi \end{aligned}$$

where

$$\alpha = \frac{\sqrt{2n_2 k_z k_\perp P}}{(2\pi)^{1/4}}$$

instead of $\alpha = 1$ as in the above rescaling.

2.1. Multiple scales analysis and amplitude equations

Exploiting the fact that $N^{-1} \ll 1$, we make the following ansatz for an asymptotic expansion of the solution

$$\begin{aligned} u(x, y; z) &= u_0(X, Y, Z_1, Z_2) + \frac{1}{N}u_1(X, Y, Z_1, Z_2) \\ &\quad + \frac{1}{N^2}u_2(X, Y, Z_1, Z_2) + \cdots. \end{aligned} \tag{2.5}$$

Furthermore, we assume that the first order contribution u_0 is of the form of a linear conical superposition, but with slowly varying amplitudes. Thus, we put

$$\begin{aligned} &u_0(X, Y, Z_1, Z_2) \\ &= \int_0^{2\pi} A_\phi(X, Y, Z_1, Z_2)\,e^{ia(x\cos(\phi)+y\sin(\phi))}\,\mathrm{d}\phi\,e^{-ia^2z} \end{aligned} \tag{2.6}$$

where the slowly varying amplitudes depend on the variables

$$X = x/N, \qquad Y = y/N, \qquad Z_1 = 2az/N, \qquad Z_2 = z/N^2. \tag{2.7}$$

Next, we combine Eq. (2.5) with (2.6) and plug into the governing PDE in (2.3). For the present paper we assume that the strength of the nonlinearity is of order $\epsilon = O(1/N)$. Then, by Remark 2.2, we can set $\epsilon = 1/N$ without loss of generality. In what follows, we also assume that the initial condition is $J_0(ar)e^{-r^2/N^2}$ i.e we choose $\alpha = 2\pi$. This choice simplifies the algebra, although the conclusions we draw and the multiple scale approach we develop are also valid for any choice of α which is $O(1)$ as $N \to \infty$.

Collecting the coefficients of powers of $1/N$ we obtain the following amplitude equations.

Order $O(1/N)$:

$$\int_0^{2\pi} \left(\frac{\partial A_\phi}{\partial Z_1} + \cos(\phi)\frac{\partial A_\phi}{\partial X} + \sin(\phi)\frac{\partial A_\phi}{\partial Y} - \frac{i}{2a}|u_0|^2 A_\phi \right) \times e^{ia(x\cos(\phi)+y\sin(\phi))}\,\mathrm{d}\phi = 0. \tag{2.8}$$

Order $O(1/N^2)$:

$$\int_0^{2\pi} \left(i\frac{\partial A_\phi}{\partial Z_2} + \frac{\partial^2 A_\phi}{\partial X^2} + \frac{\partial^2 A_\phi}{\partial Y^2} \right) e^{ia(x\cos(\phi)+y\sin(\phi))}\,\mathrm{d}\phi e^{-ia^2 z} + i\frac{\partial u_1}{\partial Z_1} + 2|u_0|^2 u_1 + {u_0}^2 u_1^* = 0. \tag{2.9}$$

Remark 2.3. (i) Observe that the above scheme can be continued, at least formally, to arbitrary orders of $1/N$.

(ii) With the assumption $\epsilon = O(1/N)$, the nonlinearity enters the amplitude equations as soon as possible for a weak nonlinearity within our framework. We also avoid tautologies since, for example, the choice $\epsilon = O(1/N^2)$ would reproduce a cubic NLS for the nonlinear amplitude equations at order $O(1/N^2)$ while we would recover the linear equations at order $O(1/N)$.

2.2. Asymptotic solutions based on amplitude equations

We observe that (2.8) holds if

$$\frac{\partial A_\phi}{\partial Z_1} = -\cos(\phi)\frac{\partial A_\phi}{\partial X} - \sin(\phi)\frac{\partial A_\phi}{\partial Y} + \frac{i}{2a}|u_0|^2 A_\phi \tag{2.10}$$

for all $\phi \in [0, 2\pi]$. Next, we derive asymptotic solutions to the nonlinear amplitude equations in (2.10) and the corresponding linearization. These will be the starting point for the derivation of several uniform estimates that compare asymptotic solutions to the ideal Bessel beam as well as the ideal Bessel beam apodized with a Gaussian.

2.2.1. Linear amplitude equations

We consider first the linearization of Eq. (2.10) given by

$$\frac{\partial A_\phi}{\partial Z_1} = -\cos(\phi)\frac{\partial A_\phi}{\partial X} - \sin(\phi)\frac{\partial A_\phi}{\partial Y} \tag{2.11}$$

which corresponds to the linear Schrödinger equation ($\epsilon = 0$) as the governing equation. From (2.11) we conclude that

$$A_\phi(X, Y, Z_1) = \tilde{A}_\phi(X - \cos(\phi)Z_1, Y - \sin(\phi)Z_1). \tag{2.12}$$

Since $A_\phi(X, Y, Z_1 = 0) = \tilde{A}_\phi(X, Y) = e^{-(X^2+Y^2)}$ we obtain in the linear case the solution

$$A_\phi(X, Y, Z_1) = e^{-\left((X-2a\cos(\phi)Z_1)^2+(Y-2a\sin(\phi)Z_1)^2\right)}, \tag{2.13}$$

and hence Eq. (2.5) yields

$$u \approx \tilde{u}_{\mathrm{lin}} = \int_0^{2\pi} e^{-\left((X-2a\cos(\phi)Z_1)^2+(Y-2a\sin(\phi)Z_1)^2\right)} \times e^{ia(x\cos(\phi)+y\sin(\phi))}\,\mathrm{d}\phi\, e^{-ia^2 z}. \tag{2.14}$$

2.2.2. Characteristic variables

Observe that in (2.12) we have introduced characteristics variables

$$\xi = X - \cos(\phi)Z_1 \quad \text{and} \quad \zeta = Y - \sin(\phi)Z_1.$$

If we consider A_ϕ along a characteristic curve $(X(s), Y(s), Z_1(s))$, parametrized by $s \geq 0$, we obtain that

$$\frac{\mathrm{d}}{\mathrm{d}s}A_\phi(X(s), Y(s), Z_1(s)) = \dot{X}\frac{\partial A_\phi}{\partial X} + \dot{Y}\frac{\partial A_\phi}{\partial Y} + \dot{Z}_1\frac{\partial A_\phi}{\partial Z_1}.$$

Thus, we put

$$\dot{Z}_1 = 1, \qquad \dot{X} = \cos(\phi), \quad \text{and} \quad \dot{Y} = \sin(\phi).$$

From the above we conclude that

$$Z_1 = s, \qquad X = X_0 + \cos(\phi)s, \quad \text{and} \quad Y = Y_0 + \sin(\phi)s$$

where (X_0, Y_0) is the starting point of the characteristic line.

2.2.3. Nonlinear amplitude equations

For the full (i.e. nonlinear) amplitude equations (2.10), we obtain similarly to the previous discussion in Sections 2.2.1 and 2.2.2 that along a characteristic curve

$$\frac{\mathrm{d}}{\mathrm{d}s}A_\phi(X(s), Y(s), Z_1(s)) = i|u_0(X(s), Y(s), Z_1(s))|^2 A_\phi(X(s), Y(s), Z_1(s))$$

holds. Hence, we conclude that A_ϕ is determined *implicitly* by

$$A_\phi(s) = A_\phi(0)\, e^{i\int_0^s |u_0(s')|^2\,\mathrm{d}s'} = e^{-({X_0}^2+{Y_0}^2)}\, e^{i\int_0^s |u_0(X_0+\cos(\phi)s', Y_0+\sin(\phi)s', s')|^2\,\mathrm{d}s'}$$

since we recall from (2.6) that the conical superposition u_0 depends on the slowly varying amplitudes. Returning to the original Cartesian coordinates the above yields

$$A_\phi(X, Y, Z_1) = e^{-((X-\cos(\phi)Z_1)^2+(Y-\sin(\phi)Z_1)^2)} \times e^{i\int_0^{Z_1} |u_0(X-\cos(\phi)Z_1+\cos(\phi)s', Y-\sin(\phi)Z_1+\sin(\phi)s', s')|^2\,\mathrm{d}s'}.$$

Hence, using the conical superposition assumption (2.6) for u_0 we obtain the asymptotic solution

$$u \approx u_{\mathrm{nl}} = e^{-ia^2 z}\int_0^{2\pi} \mathrm{d}\phi\, e^{-\left((X-2a\cos(\phi)Z_1)^2+(Y-2a\sin(\phi)Z_1)^2\right)} \times e^{ia(x\cos(\phi)+y\sin(\phi))} \times e^{i\int_0^{2az/N} |u_0((X-2a\cos(\phi)Z_1)+\cos(\phi)s', (Y-2a\sin(\phi)Z_1)+\sin(\phi)s', s')|^2\,\mathrm{d}s'}. \tag{2.15}$$

3. Main results

3.1. Linear Bessel and Bessel–Gauß beams

We start by considering the linear part of Eq. (2.3), which corresponds to the case $\epsilon = 0$. We put for brevity

$$p_\phi(x, y) := x\cos\phi + y\sin\phi. \tag{3.1}$$

For the corresponding linear IVP (2.3) with $\epsilon = 0$, (2.4) it is straight forward to check that we obtain solutions of the form

$$\int_0^{2\pi} A(\phi)e^{ia(x\cos(\phi)+y\sin(\phi))}\,\mathrm{d}\phi\, e^{-ia^2 z}. \tag{3.2}$$

Here the functions $A(\phi)$ denote the (possibly complex) amplitudes of the plane wave components of a conical superposition. We

introduce the following notation for ideal zeroth order Bessel beams

$$u_\infty = \int_0^{2\pi} e^{iap_\phi(x,y)}\,\mathrm{d}\phi\, e^{-ia^2z} = 2\pi J_0\left(a\sqrt{x^2+y^2}\right) e^{-ia^2z}. \tag{3.3}$$

Recall that we have already derived amplitude equations (2.11) and corresponding asymptotic solutions (2.14) in Section 2 using a slowly varying amplitude approach.

3.1.1. Asymptotic linear Bessel–Gauß beams

Recall that we found in Eq. (2.14) the asymptotic solution given by

$$\tilde{u}^{(1)}_{\mathrm{lin}} = \left(\int_0^{2\pi} e^{-(X-\cos(\phi)Z_1)^2} e^{-(Y-\sin(\phi)Z_1)^2} e^{iap_\phi(x,y)}\,\mathrm{d}\phi\right) e^{-ia^2z}. \tag{3.4}$$

Using the Taylor expansion of the exponential function we obtain a second approximation given by

$$\tilde{u}^{(2)}_{\mathrm{lin}} = \underbrace{\left(\int_0^{2\pi} e^{iap_\phi(x,y)}\,\mathrm{d}\phi\right) e^{-ia^2z}}_{u_\infty(x,y,z)} + \left(\int_0^{2\pi} \big((X-\cos(\phi)Z_1)^2(Y-\sin(\phi)Z_1)^2 - (X-\cos(\phi)Z_1)^2 - (Y-\sin(\phi)Z_1)^2\big) e^{iap_\phi(x,y)}\mathrm{d}\phi\right) e^{-ia^2z}. \tag{3.5}$$

Remark 3.1. Note that the first term in the expression for $\tilde{u}^{(2)}_{\mathrm{lin}}$ in Eq. (3.5) coincides with the ideal Bessel beam u_∞ in (3.3).

3.1.2. Estimates for asymptotic Bessel–Gauß beams

Next we will state and prove some uniform estimates for asymptotic solutions that provide bounds for the deviation from the ideal conical wave solutions and the apodized initial condition. In particular, from the characteristic lines we will obtain cone segments as the regions where these estimates are valid. The conical regions in our estimates are in good agreement with the Bessel regions depicted in Figs. 1(b) and 2. However, rigorous estimates may only hold on segments and not over the whole conical region.

The observation in Remark 3.1 suggests to look for estimates of the absolute error

$$|u_\infty(x,y,z) - \tilde{u}^{(2)}_{\mathrm{lin}}(x,y,z)|,$$

to compare the behavior of the approximate Bessel–Gauß beam to the ideal Bessel beam. It follows from Eqs. (3.3) and (3.5) that

$$|u_\infty - \tilde{u}^{(2)}_{\mathrm{lin}}| \le 2\pi\left((|X|+Z_1)^2 + (|Y|+Z_1)^2\right) + 2\pi(|X|+Z_1)^2(|Y|+Z_1)^2. \tag{3.6}$$

To estimate the terms $(|X|+Z_1)^2+(|Y|+Z_1)^2$ and $(|X|+Z_1)^2(|Y|+Z_1)^2$ in (3.6) we consider now the solid cone

$$\mathcal{C}^{(1)}_{N,a} := \left\{(x,y,z) : \sqrt{x^2+y^2} \le 2az\right\}. \tag{3.7}$$

For $\epsilon > 0$ and $(x,y,z) \in \mathcal{C}^{(1)}_{N,a}$ we have

$$\frac{|x|+2az}{N} \le \frac{\sqrt{x^2+y^2}+2az}{N} \le \frac{4az}{N} \le \sqrt{\epsilon} \tag{3.8}$$

where the right-hand side holds if

$$z \le z_\epsilon = \frac{\sqrt{2\epsilon}N}{8a}. \tag{3.9}$$

Similarly, we also find that

$$\frac{|y|+2az}{N} \le \frac{\sqrt{x^2+y^2}+2az}{N} \le \frac{4az}{N} \le \sqrt{\epsilon} \tag{3.10}$$

if (3.9) is satisfied. Therefore, we have

$$(|X|+Z_1)^2 \le \frac{\epsilon}{4\pi} \quad \text{and} \quad (|Y|+Z_1)^2 \le \frac{\epsilon}{4\pi} \tag{3.11}$$

if $(x,y,z) \in \mathcal{C}^{(1)}_{N,a}(\epsilon)$ where we denote by

$$\mathcal{C}^{(1)}_{N,a}(\epsilon) := \left\{(x,y,z) : \sqrt{x^2+y^2} \le 2az,\ z \le \frac{\sqrt{\epsilon}N}{8a\sqrt{\pi}}\right\} \tag{3.12}$$

the segment of $\tilde{C}_{N,a}$ bounded by the plane $\{(x,y,\pi^{-1/2}z_\epsilon)\}$. From the previous observations we obtain a uniform estimate for the right-hand side of (3.6).

Theorem 3.1. *Let $\epsilon > 0$. Then for all $(x,y,z) \in \mathcal{C}^{(1)}_{N,a}(\epsilon)$ we have*

$$|u_\infty - \tilde{u}^{(2)}_{lin}| \le \epsilon + \frac{\epsilon^2}{8\pi}. \tag{3.13}$$

Proof. It follows from (3.6) and (3.11) that

$$|u_\infty - \tilde{u}^{(2)}_{\mathrm{lin}}| \le 2\pi\frac{1}{2\pi}\epsilon + 2\pi\frac{\epsilon^2}{16\pi^2} = \epsilon + \frac{\epsilon^2}{8\pi}. \quad \square$$

Similarly to Theorem 3.1 we can estimate the deviation of an asymptotic solution from the apodized ideal solution. To do so, we approximate the asymptotic solution in (3.4) by

$$\tilde{u}^{(3)}_{\mathrm{lin}}(x,y,z) = \left(\int_0^{2\pi} e^{-(X^2+Y^2)} e^{iap_\phi(x,y)}\,\mathrm{d}\phi\right) e^{-ia^2z} + \left(\int_0^{2\pi} e^{-(X^2+Y^2)}\left(2p_\phi(X,Y)Z_1 - {Z_1}^2\right) e^{iap_\phi(x,y)}\,\mathrm{d}\phi\right) e^{-ia^2z}. \tag{3.14}$$

Thus, we obtain the estimate

$$|\tilde{u}^{(3)}_{\mathrm{lin}} - e^{(x^2+y^2)/N^2}u_\infty| \le 2\pi\left|2\max_{\phi\in[0,2\pi]}(X\cos\phi + Y\sin\phi) - Z_1\right| Z_1. \tag{3.15}$$

Case 1: Consider the cone

$$\mathcal{C}^{(2)}_{N,a} := \left\{(x,y,z) : \sqrt{x^2+y^2} \le az\right\}. \tag{3.16}$$

Then we obtain from (3.15) the inequality

$$|2(X\cos\phi + Y\sin\phi) - Z_1| \le \frac{4az}{N} \tag{3.17}$$

for $(x,y,z) \in \mathcal{C}^{(2)}_{N,a}$. Furthermore, we conclude from (3.15) and (3.17) that

$$2\pi\left|2\max_{\phi\in[0,2\pi]}(X\cos\phi + Y\sin\phi) - Z_1\right| Z_1 \le \frac{4\pi}{N^2}(2az)^2 \le \epsilon \tag{3.18}$$

when

$$z \le \frac{N\sqrt{\epsilon}}{4a\sqrt{\pi}}.$$

Hence, we put

$$\mathcal{C}^{(2)}_{N,a}(\epsilon) := \left\{(x,y,z) : \sqrt{x^2+y^2} \le az, z \le \frac{N\sqrt{\epsilon}}{4a\sqrt{\pi}}\right\}. \tag{3.19}$$

With the above observations we can now state the following theorem.

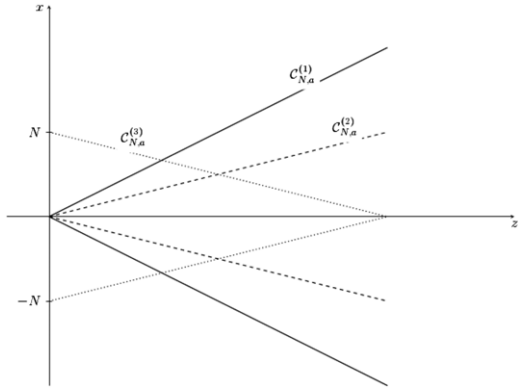

Fig. 3. The geometry of the conical regions $\mathcal{C}^{(1)}_{N,a}$ (solid lines), $\mathcal{C}^{(2)}_{N,a}$ (dashed lines), and $\mathcal{C}^{(3)}_{N,a}$ (dotted lines). The uniform estimates stated in Section 3 are valid on segments of these regions. The estimates compare an asymptotic solution to an ideal nondiffracting solution u_∞; see (3.3), or an apodized nondiffracting solution $e^{-x^2/N^2}u_\infty$. Note the common features of the geometry above and the geometries of the Bessel regions shown in Figs. 1(b) and 2 and discussed in Section 1.

Theorem 3.2. *Let $\epsilon > 0$. Then for all $(x, y, z) \in \mathcal{C}^{(2)}_{N,a}(\epsilon)$ we have*

$$|e^{-(x^2+y^2)/N^2}u_\infty - \tilde{u}^{(3)}_{lin}| \le \epsilon. \tag{3.20}$$

Proof. The statement in (3.20) follows immediately from (3.15) and (3.18). □

Case 2: Now we consider the cone

$$\mathcal{C}^{(3)}_{N,a} := \left\{(x, y, z) : \sqrt{x^2 + y^2} \le N - az\right\} \tag{3.21}$$

and the segment

$$\mathcal{C}^{(3)}_{N,a}(\epsilon) := \left\{(x, y, z) : \sqrt{x^2 + y^2} \le N - az, z \le \frac{N\epsilon}{8a\pi}\right\}. \tag{3.22}$$

We obtain the following estimate.

Theorem 3.3. *Let $\epsilon > 0$. Then for all $(x, y, z) \in \mathcal{C}^{(3)}_{N,a}(\epsilon)$ we have*

$$|e^{-(x^2+y^2)/N^2}u_\infty - \tilde{u}^{(3)}_{lin}| \le \epsilon. \tag{3.23}$$

Proof. The statement in (3.23) follows immediately from (3.15) and the fact that

$$\left|2 \max_{\phi\in[0,2\pi]} (X\cos\phi + Y\sin\phi) - Z_1\right| \le 2Z_1. \quad \square$$

The geometry of the conical regions that are considered in the above estimates is illustrated in Fig. 3. At this point we emphasize the striking resemblance to the geometries of the Bessel regions discussed in Section 1; see Figs. 1 and 2.

Remark 3.2 (*Group Versus Phase Velocity*)**.** Note that in Theorem 3.1 the boundaries of the cone changed in the transverse directions at a rate equal to the group velocity of the conical wave while in Theorems 3.2 and 3.3 this happens at the phase velocity. This suggests that the Bessel region may actually be larger than the geometric optics argument illustrated in Fig. 2 predicts.

3.2. Nonlinear Bessel–Gauß beams

We return in this section to the cubic nonlinear Schrödinger equation and consider again the IVP (2.3), (2.4), but now with $\epsilon > 0$. Recall that we have already derived amplitude equations (2.10) and asymptotic solutions (2.15) for this case in Section 2.

Since in this paper we are primarily interested in weak nonlinearities we assume that the nonlinearity introduces only a small perturbation into the linear system. Hence, we use the previously found linear solutions to express the nonlinear $|u|^2$ term up to order $1/N$. In particular, if we omit the phase modulation arising from the nonlinearity in (2.15) we recover the linear asymptotic solution (2.14). Thus, we linearize the NLS (2.3) by using the linear solution or a linear asymptotic solution from (2.14), (3.4), or (3.5). Thus, we obtain the following possible expressions for the nonlinearity.

$$F = |\tilde{u}_{\text{lin}}|^2, \qquad \tilde{F} = |\tilde{u}^{(1)}_{\text{lin}}|^2, \qquad \tilde{\tilde{F}} = |\tilde{u}^{(2)}_{\text{lin}}|^2. \tag{3.24}$$

In the present paper we focus on nonlinearity which enters in the amplitude equations at order $1/N$, and in the upcoming discussion we employ the last term in (3.24) to keep our analysis tractable. We believe however, that our arguments can be extended even to the nonlinear situation.

Combining one of the above expressions with Eq. (2.3) we obtain an equation of the form

$$\frac{\partial}{\partial t}u(x, y, z) = \Delta_{x,y}u(x, y, z) \pm \epsilon F_{nl}(x, y, z)u(x, y, z) \tag{3.25}$$

where $F_{nl}(X, Y, Z_1) = F$, $\tilde{F}$, or $\tilde{\tilde{F}}$ as defined in (3.24). In particular, the amplitude equation derived in (2.10) takes the form

$$\begin{aligned}\frac{\partial A_\phi}{\partial Z_1}(X, Y, Z_1, Z_2) = &-\cos(\phi)\frac{\partial A_\phi}{\partial X}(X, Y, Z_1, Z_2)\\ &-\sin(\phi)\frac{\partial A_\phi}{\partial Y}(X, Y, Z_1, Z_2)\\ &\pm i\frac{1}{2a}f_{nl}(X, Y, Z_1)A_\phi(X, Y, Z_1, Z_2)\end{aligned} \tag{3.26}$$

where we express the term F_{nl} in the slow variables as $f_{nl}(X, Y, Z_1)$.

3.2.1. Asymptotic nonlinear Bessel–Gauß beams

We obtain the following asymptotic solution for the nonlinear IVP

$$\begin{aligned}\tilde{u}^{(0)}_{\text{nl}} = {} & e^{-ia^2t}\int_0^{2\pi} e^{-(X-Z_1\cos(\phi))^2}e^{-(Y-Z_1\sin(\phi))^2}e^{ia(x\cos(\phi)+y\sin(\phi))}\\ & \times e^{\pm i\int_0^{Z_1} f_{nl}(X-Z_1\cos(\phi)+\sigma\cos(\phi),Y-Z_1\sin(\phi)+\sigma\sin(\phi),\sigma)\,\mathrm{d}\sigma}\,\mathrm{d}\phi.\end{aligned} \tag{3.27}$$

Using the Taylor series of the exponential function we obtain

$$\begin{aligned}\tilde{u}^{(1)}_{\text{nl}} = {} & \underbrace{\int_0^{2\pi} e^{-(X-Z_1\cos(\phi))^2}e^{-(Y-Z_1\sin(\phi))^2}e^{ia(x\cos(\phi)+y\sin(\phi))}\,\mathrm{d}\phi\, e^{-ia^2t}}_{\tilde{u}_{\text{lin}}(x,t)}\\ & \pm i\int_0^{2\pi} e^{-(X-Z_1\cos(\phi))^2}e^{-(Y-Z_1\sin(\phi))^2}e^{ia(x\cos(\phi)+y\sin(\phi))}\\ & \times\left(\int_0^{Z_1} f_{nl}(X+(\sigma-Z_1)\cos(\phi), Y+(\sigma-Z_1)\sin(\phi), \sigma)\,\mathrm{d}\sigma\right)\\ & \times \mathrm{d}\phi\, e^{-ia^2t}.\end{aligned} \tag{3.28}$$

Furthermore, we also obtain

$$\begin{aligned}\tilde{u}^{(2)}_{\text{nl}} = {} & \underbrace{\int_0^{2\pi} e^{ia(x\cos(\phi)+y\sin(\phi))}\,\mathrm{d}\phi\, e^{-ia^2z}}_{u_\infty(x,t)}\\ & -\int_0^{2\pi}(X-Z_1\cos(\phi))^2e^{ia(x\cos(\phi)+y\sin(\phi))}\,\mathrm{d}\phi\, e^{-ia^2z}\\ & -\int_0^{2\pi}(Y-Z_1\sin(\phi))^2e^{ia(x\cos(\phi)+y\sin(\phi))}\,\mathrm{d}\phi\, e^{-ia^2z}\end{aligned}$$

$$+\int_0^{2\pi}(X-Z_1\cos(\phi))^2(Y-Z_1\sin(\phi))^2 \times e^{ia(x\cos(\phi)+y\sin(\phi))}\,\mathrm{d}\phi\,e^{-ia^2z} \pm i\int_0^{2\pi}(1-(X-Z_1\cos(\phi))^2)(1-(Y-Z_1\sin(\phi))^2) \times\left(\int_0^{Z_1} f_{nl}(X+(\sigma-Z_1)\cos(\phi),Y + (\sigma-Z_1)\sin(\phi),\sigma)\,\mathrm{d}\sigma\right) \times e^{ia(x\cos(\phi)+y\sin(\phi))}\,\mathrm{d}\phi\,e^{-ia^2z}. \tag{3.29}$$

3.2.2. Uniform estimates

If we consider Eq. (3.25) with $F_{nl}=\tilde{\tilde{F}}$ then we can find estimates relating the linear and nonlinear solutions. First we make the following observation.

Remark 3.3. Observe that for $F_{nl}=\tilde{\tilde{F}}$ as defined in (3.24) we have

$$\tilde{\tilde{F}}=|\tilde{u}^{(2)}_{\mathrm{lin}}|^2\le\left(2\pi+\int_0^{2\pi}(X+Z_1)^2\,\mathrm{d}\phi+\int_0^{2\pi}(Y+Z_1)^2\,\mathrm{d}\phi + \int_0^{2\pi}(X+Z_1)^2(Y+Z_1)^2\,\mathrm{d}\phi\right)^2.$$

Hence, for all (x,y,z) contained in the cone segment

$$\mathcal{C}^{(1)}_{N,a}(\epsilon):=\left\{(x,y,z):\sqrt{x^2+y^2}\le 2az,\ z\le\frac{\sqrt{\epsilon}N}{8a\sqrt{\pi}}\right\} \tag{3.30}$$

we have $(X+Z_1)^2\le\epsilon/(4\pi)$ and $(Y+Z_1)^2\le\epsilon/(4\pi)$. We obtain thus

$$|\tilde{u}^{(2)}_{\mathrm{lin}}|^2\le\left(2\pi+\epsilon+\frac{\epsilon^2}{8\pi}\right)^2.$$

With the observations made in Remark 3.3, we obtain the following estimate.

Theorem 3.4. *Let $\epsilon>0$. Then for all (x,y,z) in the solid cone segment $\mathcal{C}^{(1)}_{N,a}(\epsilon)$ we have the following estimates*

(i)

$$|\tilde{u}_{\mathrm{lin}}-\tilde{u}^{(1)}_{\mathrm{nl}}|\le\frac{\sqrt{\pi}}{2}\sqrt{\epsilon}\left(2\pi+\epsilon+\frac{\epsilon^2}{8\pi}\right)^2=\pi^{3/2}\sqrt{\epsilon}+o(\epsilon),$$

(ii)

$$|u_\infty-\tilde{u}^{(2)}_{\mathrm{nl}}|\le\frac{\sqrt{\pi}}{2}\sqrt{\epsilon}\left(2\pi+\epsilon+\frac{\epsilon^2}{8\pi}\right)^2+\epsilon+\frac{\epsilon^2}{8\pi} =\epsilon+\pi^{3/2}\sqrt{\epsilon}+o(\epsilon).$$

Proof. (i) Combining (3.4) and (3.28) we obtain

$$|\tilde{u}_{\mathrm{lin}}-\tilde{u}^{(1)}_{\mathrm{nl}}|\le\int_0^{2\pi}\left(\int_0^{Z_1}|f_{nl}(X+(\sigma-Z_1)\cos(\phi),Y + (\sigma-Z_1)\sin(\phi),\sigma)|\,\mathrm{d}\sigma\right)\mathrm{d}\phi.$$

From the above considerations and Remark 3.3 we obtain

$$|\tilde{u}_{\mathrm{lin}}-\tilde{u}^{(1)}_{\mathrm{nl}}|\le 2\pi\frac{2a}{N}\frac{\sqrt{\epsilon}N}{8a\sqrt{\pi}}\left(2\pi+\epsilon+\frac{\epsilon^2}{8\pi}\right)^2 =\frac{\sqrt{\pi}}{2}\sqrt{\epsilon}\left(2\pi+\epsilon+\frac{\epsilon^2}{8\pi}\right)^2.$$

(ii) To show that the second statement holds, we consider

$$|u_\infty-\tilde{u}^{(2)}_{\mathrm{nl}}|\le\int_0^{2\pi}(X-Z_1\cos(\phi))^2\,\mathrm{d}\phi + \int_0^{2\pi}(Y-Z_1\sin(\phi))^2\,\mathrm{d}\phi + \int_0^{2\pi}(X-Z_1\cos(\phi))^2(Y-Z_1\sin(\phi))^2\,\mathrm{d}\phi + \int_0^{2\pi}\int_0^{Z_1}\left|f_{nl}(X_{\sigma,\phi},Y_{\sigma,\phi},\sigma)\right|\,\mathrm{d}\sigma\,\mathrm{d}\phi.$$

Here we denote $X_{\sigma,\phi}=X+(\sigma-Z_1)\cos(\phi)$, $Y_{\sigma,\phi}=Y+(\sigma-Z_1)\sin(\phi)$. From the previous observations and Remark 3.3 we obtain – similarly to the proof of (i) – the following

$$|u_\infty-\tilde{u}^{(2)}_{\mathrm{nl}}|\le\epsilon+\frac{\epsilon^2}{8\pi}+\frac{\sqrt{\pi}}{2}\sqrt{\epsilon}\left(2\pi+\epsilon+\frac{\epsilon^2}{8\pi}\right)^2.\quad\square$$

Next, we consider the asymptotic solution

$$\tilde{u}^{(3)}_{\mathrm{nl}}=e^{-ia^2z}\left(e^{-(X^2+Y^2)}\int_0^{2\pi}e^{iap_\phi(x,y)}\,\mathrm{d}\phi + e^{-(X^2+Y^2)}\int_0^{2\pi}\left(2\frac{p_\phi(x,y)}{N}-Z_1\right)Z_1e^{iap_\phi(x,y)}\,\mathrm{d}\phi \pm ie^{-(X^2+Y^2)}\int_0^{2\pi}\left(1+2\frac{p_\phi(x,y)}{N}Z_1-{Z_1}^2\right) \times\int_0^{Z_1}f_{nl}(X_{\sigma,\phi},Y_{\sigma,\phi},\sigma)\,\mathrm{d}\sigma e^{iap_\phi(x,y)}\,\mathrm{d}\phi\right). \tag{3.31}$$

Note that the right-hand side term in the first line of (3.31) corresponds to the apodized ideal solution while we recover the linear asymptotic solution (3.14) from the first and second lines. This suggests to look for uniform estimates of

$$|\tilde{u}^{(3)}_{\mathrm{nl}}-e^{-(x^2+y^2)/N^2}u_\infty| \tag{3.32}$$

and

$$|\tilde{u}^{(3)}_{\mathrm{nl}}-\tilde{u}^{(3)}_{\mathrm{lin}}|. \tag{3.33}$$

Case 1: Consider again the cone $\mathcal{C}^{(2)}_{N,a}$ as well as the segment $\mathcal{C}^{(2)}_{N,a}(\epsilon)$ defined in (3.16) and (3.19), respectively. Moreover, we define

$$\mathcal{C}^{(2')}_{N,a}(\epsilon):=\left\{(x,y,z)\in\mathcal{C}^{(2)}_{N,a}:z\le\frac{N\sqrt{\epsilon}}{8a\sqrt{\pi}}\right\}. \tag{3.34}$$

In analogy to Theorem 3.2 we state the following.

Theorem 3.5. *Let $\epsilon>0$. Then for all $(x,y,z)\in\mathcal{C}^{(2')}_{N,a}(\epsilon)$ we have*

(i)

$$|e^{-(x^2+y^2)/N^2}u_\infty-\tilde{u}^{(3)}_{\mathrm{nl}}|\le\epsilon+\frac{\sqrt{\pi}}{2}\sqrt{\epsilon}+o(\epsilon), \tag{3.35}$$

(ii)

$$|\tilde{u}^{(3)}_{\mathrm{nl}}-\tilde{u}^{(3)}_{\mathrm{lin}}|\le\frac{\sqrt{\pi}}{2}\sqrt{\epsilon}+o(\epsilon). \tag{3.36}$$

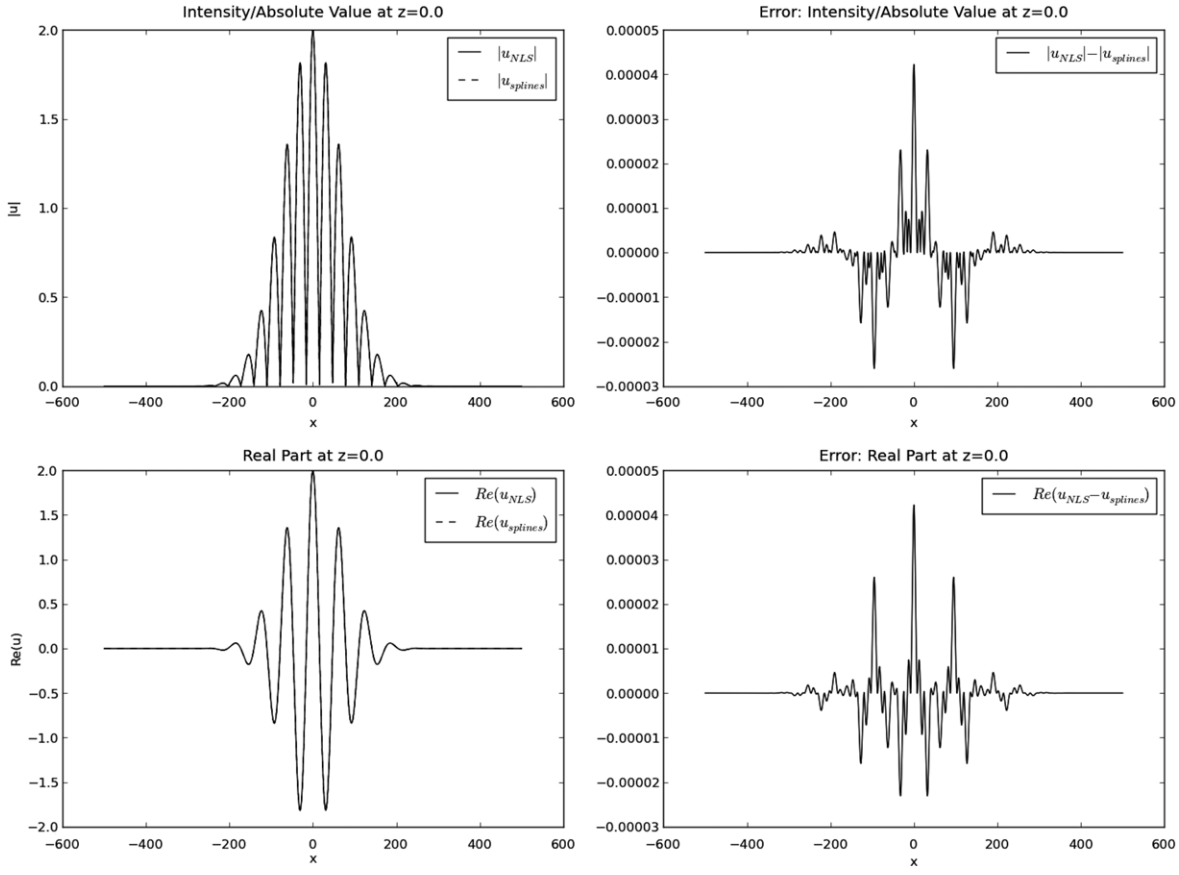

Fig. 4. Plots of the initial conditions ($z = 0.0$) for a comparison of numerical solutions for NLS and amplitude equations (top left: absolute value/intensity, bottom left: real part, top and bottom right: absolute error between absolute value and real part of the NLS and asymptotic solution, respectively). Here u_{NLS} denotes the solution of the NLS equation while we solve the amplitude equations on a coarser grid and use cubic spline interpolation to compute the asymptotic solution u_{spline}.

Proof. The statements follow from (3.18) and Remark 3.3. □

Case 2: Now we recall the definition of $\mathcal{C}^{(3)}_{N,a}$ and $\mathcal{C}^{(3)}_{N,a}(\epsilon)$ in (3.21) and (3.22), respectively. We put

$$\mathcal{C}^{(3')}_{N,a}(\epsilon) := \mathcal{C}^{(3)}_{N,a}(\epsilon) \cap \mathcal{C}^{(1)}_{N,a}(\epsilon). \tag{3.37}$$

We obtain the following estimate.

Theorem 3.6. *Let $\epsilon > 0$. Then for all $(x, y, z) \in \mathcal{C}^{(3')}_{N,a}(\epsilon)$ we have*

(i)

$$|e^{-(x^2+y^2)/N^2} u_\infty - \tilde{u}^{(3)}_{\mathrm{nl}}| \le \epsilon + \frac{\sqrt{\pi}}{2}\sqrt{\epsilon} + o(\epsilon), \tag{3.38}$$

(ii)

$$|\tilde{u}^{(3)}_{\mathrm{nl}} - \tilde{u}^{(3)}_{\mathrm{lin}}| \le \frac{\sqrt{\pi}}{2}\sqrt{\epsilon} + o(\epsilon). \tag{3.39}$$

Proof. The statements also follow from (3.18) and Remark 3.3. □

4. Numerical evaluation of the multiple scales approach

In this section we present the results of several numerical experiments based on an implementation of our amplitude equations. First, we discuss briefly the analogue of our multiple scales analysis in one transverse dimension (1+1D). Then we will discuss numerical experiments that compare the numerical solution obtained from our amplitude equations to the result of a standard split-step Fourier method.

4.1. Asymptotic analysis in 1+1D

Observe that the multiple scales analysis presented in Section 2 can also be used to derive amplitude equations in the case of only one transverse dimension. The appropriate IVP in this case takes the form

$$-i\frac{\partial u}{\partial z} = \frac{\partial^2 u}{\partial x^2} \pm \epsilon |u|^2 u, \tag{4.1}$$

$$u = e^{-x^2/N^2}(e^{iax} + e^{-iax}). \tag{4.2}$$

We obtain the following set of amplitude equations

$$-i\frac{\partial A_+}{\partial Z_1} = \frac{\partial A_+}{\partial X} \pm \epsilon |u_0|^2 A_+, \tag{4.3}$$

$$-i\frac{\partial A_-}{\partial Z_1} = -\frac{\partial A_-}{\partial X} \pm \epsilon |u_0|^2 A_-, \tag{4.4}$$

where the asymptotic solution is of the form

$$u(x; z) \approx A_+(X, Z_1, Z_2)\, e^{iax} + A_-(X, Z_1, Z_2)\, e^{-iax}. \tag{4.5}$$

Once we have derived our amplitude equations, we can proceed analogously to Section 3 and obtain uniform estimates similar to the 1+2D case. Although the case of two transverse dimensions appears to be more relevant in applications, the 1+1D case often provides new and important insights; see for example Berry and Balasz [23], Bandres and Gutiérrez-Vega [15], and Lotti et al. [14] for related discussions of Airy beams in 1+1D.

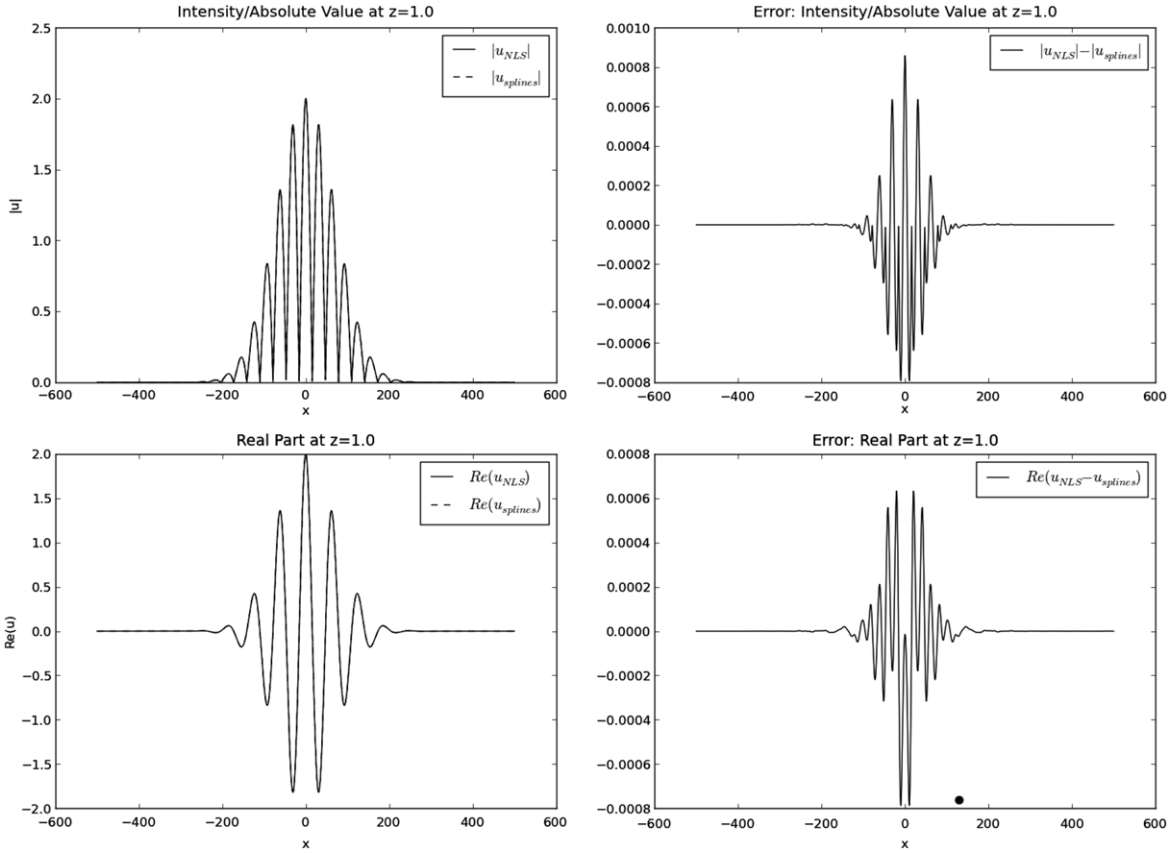

Fig. 5. Comparison of numerical solutions for NLS and amplitude equations, $z = 1.0$; u_{NLS} denotes the solution of the NLS equation while we solve the amplitude equations on a coarser grid and use cubic spline interpolation to compute the asymptotic solution u_{spline}.

4.2. Numerical experiments

For the 1+1D case we have implemented numerical solvers for the focusing NLS equation (4.1) and the corresponding amplitude equations (4.3), (4.4) using a standard split-step Fourier method. Furthermore, we solve the amplitude equations on a significantly coarser grid than the NLS equation. To reconstruct the asymptotic solution (4.5) on the fine grid, we use a cubic spline interpolation method. The numerical methods were implemented in Python using the boxSciPy [27] and matplotlib [28] libraries.

Remark 4.1 (*Split-Step Fourier Method*)**.** Consider a nonlinear PDE of the form

$$-i\frac{\partial u}{\partial z} = \frac{\partial^2 u}{\partial x^2} + |u|^2 u, \tag{4.6}$$

with initial conditions

$$u(x;0) = u_0(x). \tag{4.7}$$

Then a numerical approximation of the IVP (4.6), (4.7) can be computed at $z + \Delta z$ with the following split-step scheme, starting with $u^{(0)} = u_0(x)$.

1. *Nonlinear half-step:* Solve for a step length $\frac{1}{2}\Delta z$ the nonlinear problem

   $$-i\frac{\partial u}{\partial z} = |u|^2 u.$$

   Put

   $$u^{(n+1)} = u^{(n)}\ \exp(i|u^{(n)}|^2 \Delta z/2).$$

2. *Linear full-step:* Solve for a step length Δz the linear problem

   $$-i\frac{\partial u}{\partial z} = \frac{\partial^2 u}{\partial x^2}.$$

   Put

   $$u^{(n+1)} = \mathcal{F}^{-1}[\mathcal{F}[u^{(n+1)}]\ \exp(-ik_x{}^2 \Delta z)]$$

   where $\mathcal{F}$ and $\mathcal{F}^{-1}$ denote the Fourier transform with respect to x and its inverse, respectively.
3. *Nonlinear half-step:* Solve for a step length $\frac{1}{2}\Delta z$ the nonlinear problem

   $$-i\frac{\partial u}{\partial z} = |u|^2 u.$$

   Put

   $$u^{(n+1)} = u^{(n+1)}\ \exp(i|u^{(n+1)}|^2 \Delta z/2).$$

We refer for example to Taha and Ablowitz [29], Weideman and Herbst [30] for a more detailed discussion.

In the following experiments we use a transverse grid with 2^{12} grid points in the interval $[-500, 500]$ to solve the NLS (4.1) with a split-step Fourier method (see Remark 4.1). To solve the amplitude equations we use a coarser grid with only 2^6 grid points. We interpolate between the two grids using a cubic spline interpolation method. Moreover, we fix the parameters $N = 100.0$ and $a = 0.1$. Fig. 4 shows the absolute value and real part of the initial conditions for $z = 0$ in the left column. We solve the NLS and amplitude equations for $z = 1.0, 5.0, 10.0$ numerically (left column Figs. 5–7) and compare the results (right column Figs. 5–7); see Table 1 for a summary of the propagation intervals and number of grid points.

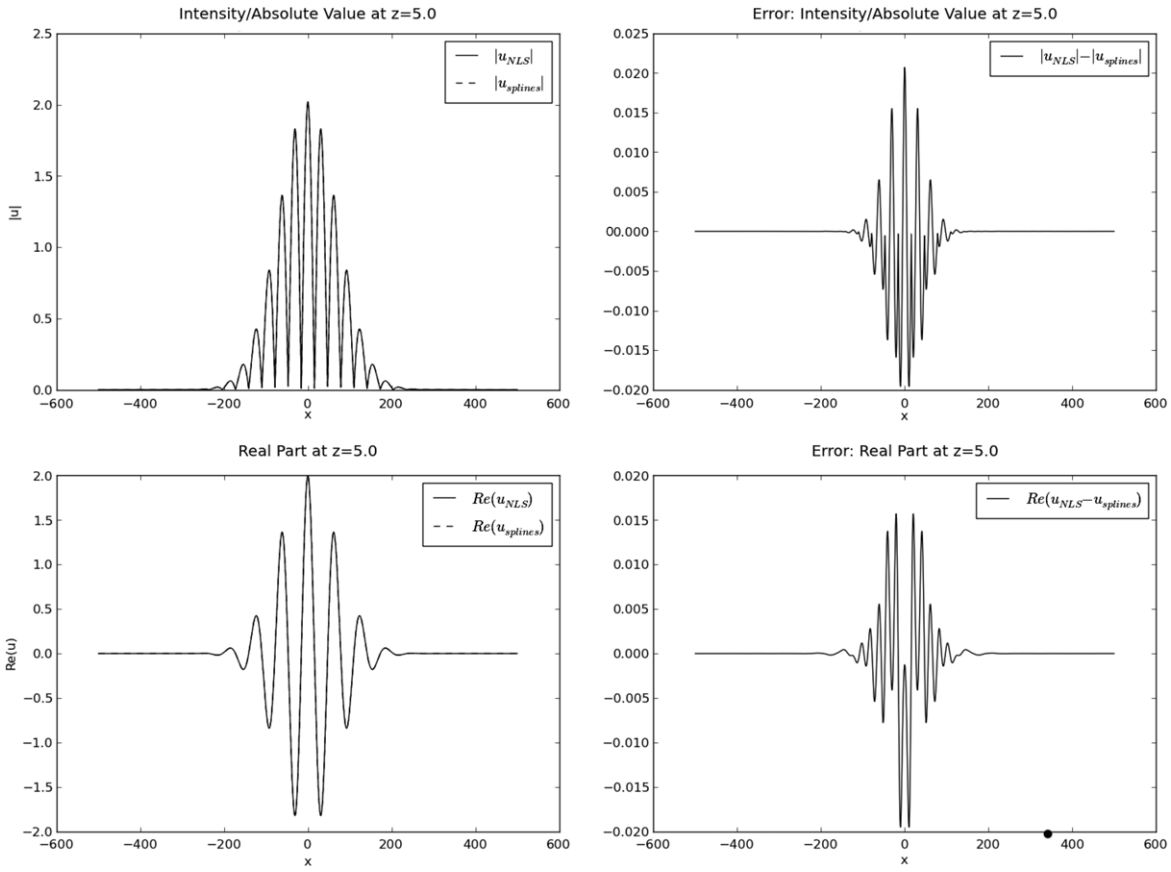

Fig. 6. Comparison of numerical solutions for NLS and amplitude equations, $z = 5.0$; u_{NLS} denotes the solution of the NLS equation while we solve the amplitude equations on a coarser grid and use cubic spline interpolation to compute the asymptotic solution u_{spline}.

Table 1
Choice of parameters for the propagation grids in the numerical experiments.

Interval (z)	Number of grid points
[0.0, 1.0]	10
[0.0, 5.0]	50
[0.0, 10.0]	100

The plots in Figs. 4–7 show that our amplitude equations can be used to compute good approximations to the real part and the absolute value (intensity) of the transverse profile. The left column contains plots of the absolute value (top) and real part (bottom) while the plots in the right column show the difference between the solution to the NLS equation and the amplitude equations. Since we use a significantly coarser grid for the amplitude equations, we do not have exact agreement for the initial conditions in Fig. 4. However, although we use only 2^6 out of 2^{12} for the amplitudes, the error between the solution of the NLS equation (u_{NLS}) and the asymptotic solution (u_{spline}) is less than $5 \cdot 10^{-5}$ if we use a cubic spline interpolation while simple linear interpolation would only allow for reduction of the coarse grids to around 2^{10} grid points. After propagating one unit in nine steps we see in Fig. 5 that the error for the real part is still at the same order of magnitude as that for the initial interpolation error in Fig. 4. After five units the maximal errors in Fig. 6 are around 2%. Even after propagating for ten units, as shown in Fig. 7, the maximal errors are well below 10%. We also point out here that changing the parameters a and N confirms that the accuracy of the approximation depends on the ratio N/a and not solely on the Gaussian width N; this dependency can also be seen directly in the uniform estimates in Section 3.

The experiments described above suggest that the amplitude equations derived in Section 3 may be useful tools for numerical simulations in the 1+2D case as well. A significant complication consists in the fact that the conical waves in 1+2D are in general not a discrete superposition but are instead generated by an uncountable family of plane waves; see for example Eq. (3.2). Thus, the need to approximate the wave vector cone by a discrete polyhedron causes a loss of accuracy and may increase the computational effort. We believe that the investigation of the aforementioned discrete conical waves may provide interesting insights into the propagation behavior of nonlinear conical waves, in particular if symmetry assumptions such as radially symmetric initial conditions, can be employed to reduce the computational effort. We plan to return to these questions in a separate paper.

5. Conclusions

Ideal Bessel beams in a linear medium are infinite energy superpositions of plane waves whose wave vectors lie on a cone. They are of great interest in optics because they are nondiffracting [5]. They also have a remarkable self-healing property. The beam can be partially obstructed on its axis, but the energy from the side lobes will feed into the center and the beam can reconstitute itself [5]. These properties are, however, a consequence of the medium being linear and the beam having infinite energy.

In this paper we investigate the question of how much of these properties carry over to physically realizable (apodized) beams with finite energy propagating in a weakly nonlinear medium. The two parameters which mainly characterize the difference between a physical beam and an ideal Bessel beam are the beam width $N \gg 1$ in terms of the wavelength, and the strength of the

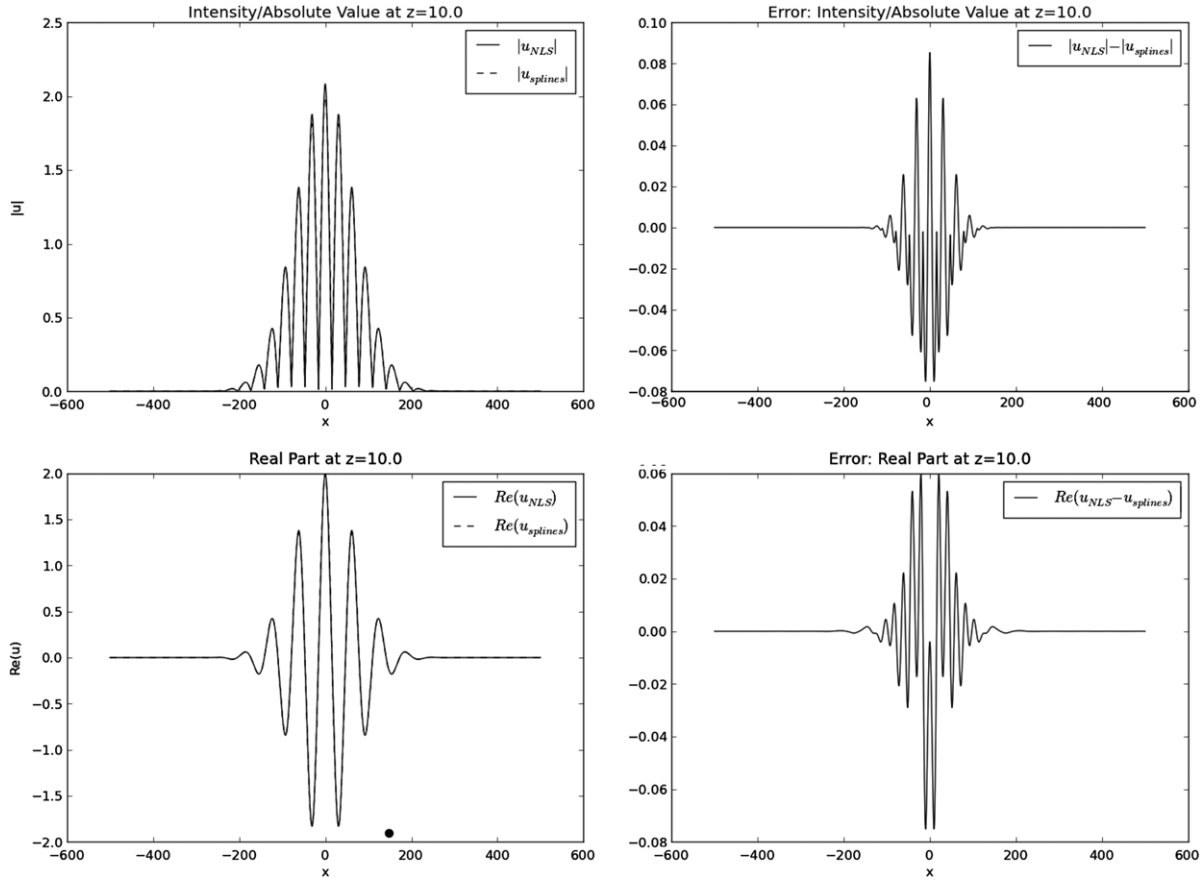

Fig. 7. Comparison of numerical solutions for NLS and amplitude equations, $z = 10.0$; u_{NLS} denotes the solution of the NLS equation while we solve the amplitude equations on a coarser grid and use cubic spline interpolation to compute the asymptotic solution u_{spline}.

nonlinearity $\epsilon \ll 1$. As $N \to \infty$ and $\epsilon \to 0$, we thus expect to recover the ideal Bessel beam in a linear medium. In this paper, we use a multiple scales method to derive amplitude equations and asymptotic solutions for the propagation of apodized conical waves under a cubic NLS with two transverse dimensions in the regime where $\epsilon \sim 1/N$.

Our analysis demonstrates that physical beams do indeed approximate the ideal Bessel beams, both in intensity and in phase, but only in finite regions that have a characteristic conical shape and whose extent depends linearly on N. This agrees with geometrical optics and experimental observations which reveal a conical *Bessel region* (see Fig. 1(b)) where the apodized beam behaves like an ideal Bessel beam.

Through our analysis, we are able to prove precise uniform estimates for asymptotic solutions in the linear and the nonlinear case that are in good qualitative agreement with experimental observations of Bessel regions. Moreover, some of these results suggest that the approximation of an ideal conical wave may actually extend into a region that is not predicted by the geometric optics description of the Bessel region.

We have focused on the case of zeroth order Bessel beams in the presentation of our uniform estimates, but we expect that these methods and results can be extended to study higher order Bessel beams and even more generally to superpositions of such beams.

The multiple scale analysis also points a way to efficient numerical simulations of these apodized beams. Directly simulating the wave equation for these beams will require a grid on the scale of the wavelength. However the amplitude equations we obtain can be solved numerically on a grid on the scale of the apodization. For $N \gg 1$, this can result in a significant increase in efficiency. We have presented numerical experiments that demonstrate this approach for the case of one transverse dimension. In ongoing work, we are trying to extend this idea to radially symmetric initial conditions in the higher dimensional case as well.

In the present paper we have studied the effects of diffraction and nonlinearity on finite energy approximations to conical waves in the context of the Nonlinear Schrödinger equation. The NLS equation is applicable to nearly monochromatic waves in the presence of a weak nonlinearity [17].

There are two natural extensions of this analysis which we hope to pursue. First, there are other types of nondiffracting beams which are not conical waves, e.g., Airy beams [23]. These beams have been studied in linear media [25,11,15]. Since Airy beams are also nearly monochromatic, we expect that our multiple-scale analysis can be extended to study the propagation of Airy beams [25], Airy–Bessel beams [11] and apodized Airy–Gauss beams [15] in weakly nonlinear media.

Another avenue for further investigation is the development of multi-scale methods for apodized ultrashort pulses. Ultrashort pulses are compressed in the time domain and thus broadband in frequency by the uncertainty principle. In this situation, one has to account for the effects of dispersion on a broadband pulse along with the effects of diffraction and weak nonlinearities. Consequently, the NLS equation is not a good model for the propagation of ultrashort pulses.

It is thus a significant challenge to extend the present work to investigate the propagation of ultrashort pulses. The study of ultrashort pulses is currently a very active field of research; see for example Alterman and Rauch [31], Balakin et al. [32], Glasner et al. [33], Kolesik et al. [34], and Schäfer and Wayne [35]. These works focus on exploiting the shortness of the pulse in the propagation direction to build multiple-scale models. Less important in

these models is the structure of the pulse in the transverse direction. We intend to include the effects of the transverse apodization into the multiple-scale models for ultrashort pulses. This is an important issue in the analysis and the numerical simulation of physically realizable, finite energy, ultrashort pulses.

Acknowledgments

This research was supported by AFOSR MURI, "Mathematical Modeling and Experimental Validation of Ultrashort Nonlinear Light–Matter Coupling associated with Filamentation in Transparent Media", grant FA9550-10-1-0561. We also thank Professors Moysey Brio, Miroslav Kolesik, and Per Jakobsen for fruitful discussions.

References

[1] Lord Rayleigh, On the passage of electric waves through tubes, or the vibrations of dielectric cylinders, Phil. Mag. 43 (1897).
[2] J. Durnin, Exact solutions for nondiffracting beams. I. The scalar theory, J. Opt. Soc. Amer. A 4 (4) (1987) 651–654.
[3] J. Durnin, J.J. Miceli, J.H. Eberly, Diffraction-free beams, Phys. Rev. Lett. 58 (15) (1987) 1499–1501.
[4] J. McLeod, The axicon: a new type of optical element, J. Opt. Soc. Amer. 44 (8) (1954) 592–597.
[5] D. McGloin, K. Dholakia, Bessel beams: diffraction in a new light, Contemp. Phys. 46 (1) (2005) 15–28.
[6] F. Gori, G. Guattari, C. Padovani, Bessel–Gauss beams, Opt. Commun. 64 (6) (1987) 491–495.
[7] P.L. Overfelt, C.S. Kenney, Comparison of the propagation characteristics of Bessel, Bessel–Gauss, and Gaussian beams diffracted by a circular aperture, J. Opt. Soc. Amer. A 8 (5) (1991) 732–745.
[8] J.C. Gutiérrez-Vega, M.A. Bandres, Helmholtz–Gauss waves, J. Opt. Soc. Amer. A 22 (2) (2005) 289–298.
[9] M.A. Bandres, M. Guizar-Sicairos, Paraxial group, Opt. Lett. 34 (2009) 13–15.
[10] T. Graf, D. Christodoulides, M. Mills, J. Moloney, S. Venkataramani, E. Wright, Propagation of Gaussian-apodized paraxial beams through first-order optical systems via complexcoordinate transforms and ray transfer matrices, J. Opt. Soc. Amer. A 29 (2012) 1860–1869.
[11] A. Chong, W.H. Renninger, D.N. Christodoulides, F.W. Wise, Airy–Bessel wave packets as versatile linear light bullets, Nature Photonics 4 (2010) 103–106.
[12] D. McGloin, V. Garcés-Chávez, K. Dholakia, Interfering Bessel beams for optical micromanipulation, Opt. Lett. 28 (8) (2003) 657–659.
[13] R. Vasilyeu, A. Dudley, N. Khilo, A. Forbes, Generating superpositions of higher-order Bessel beams, Opt. Express 17 (26) (2009) 23389–23395.
[14] A. Lotti, D. Faccio, A. Couairon, D.G. Papazoglou, P. Panagiotopoulos, D. Abdollahpour, S. Tzortzakis, Stationary nonlinear Airy beams, Phys. Rev. A 84 (2) (2011).
[15] M.A. Bandres, J.C. Gutiérrez-Vega, Airy–Gauss beams and their transformation by paraxial optical systems, Opt. Express 15 (25) (2007) 16719–16728.
[16] P. Johannisson, D. Anderson, M. Lisak, M. Marklund, Nonlinear Bessel beams, Opt. Commun. (2003) 107–115.
[17] J.V. Moloney, A.C. Newell, Nonlinear Optics, in: Advanced Book Program, Westview Press, Boulder, CO, 2004.
[18] A. Bamberger, B. Engquist, L. Halpern, P. Joly, Parabolic wave equation approximations in heterogeneous media, SIAM J. Appl. Math. 48 (1) (1988) 99–128.
[19] A. Bamberger, B. Engquist, L. Halpern, P. Joly, Higher order paraxial wave equation approximations in heterogeneous media, SIAM J. Appl. Math. 48 (1) (1988) 129–154.
[20] R. Grella, Fresnel propagation and diffraction and paraxial wave equation, J. Opt. 13 (6) (1982) 367–374.
[21] C. Sulem, P.L. Sulem, The Nonlinear Schrödinger Equation: Self-Focusing and Wave Collapse, in: Applied Mathematical Sciences, Springer, 1999.
[22] P.D. Miller, Applied Asymptotic Analysis, in: Graduate Studies in Mathematics, American Mathematical Society, 2006.
[23] M.V. Berry, N.L. Balazs, Non-spreading wave packets, Amer. J. Phys. 47 (3) (1979) 264–267.
[24] K. Dholakia, T. Cizmar, Shaping the future of manipulation, Nature Photonics 5 (2011) 335–342.
[25] G.A. Siviloglou, J. Broky, A. Dogariu, D.N. Christodoulides, Observation of accelerating Airy beams, Phys. Rev. Lett. 99 (21) (2007) 213901.
[26] G.N. Watson, A treatise on the theory of Bessel functions, in: Cambridge Mathematical Library, Cambridge University Press, Cambridge, 1995, Reprint of the second (1944) edition.
[27] E. Jones, T. Oliphant, P. Peterson, et al. SciPy: open source scientific tools for Python, 2001.
[28] J.D. Hunter, Matplotlib: a 2D graphics environment, Comput. Sci. Eng. 9 (3) (2007) 90–95.
[29] T.R. Taha, M.J. Ablowitz, Analytical and numerical aspects of certain nonlinear evolution equations. II. Numerical, nonlinear Schrödinger equation, J. Comput. Phys. 55 (2) (1984) 203–230.
[30] J.A.C. Weideman, B.M. Herbst, Split-step methods for the solution of the nonlinear Schrödinger equation, SIAM J. Numer. Anal. 23 (3) (1986) 485–507.
[31] D. Alterman, J. Rauch, Diffractive short pulse asymptotics for nonlinear wave equations, Phys. Lett. A 264 (2000) 390–395.
[32] A.A. Balakin, A.G. Litvak, V.A. Mironov, S.A. Skobelev, Structural features of the self-action dynamics of ultrashort electromagnetic pulses, J. Exp. Theor. Phys. 104 (2007) 363–378.
[33] K. Glasner, M. Kolesik, J.V. Moloney, A.C. Newell, Canonical and singular propagation of ultrashort pulses in a nonlinear medium, Int. J. Opt. (2012).
[34] M. Kolesik, J.V. Moloney, M. Mlejnek, Unidirectional optical pulse propagation equation, Phys. Rev. Lett. 89 (28) (2002) 283902.
[35] T. Schäfer, C.E. Wayne, Propagation of ultra-short pulses in cubic nonlinear media, Physica D 196 (2004) 90–105.